

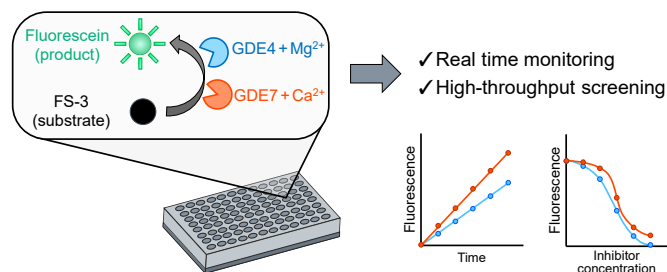
Development of a selective fluorescence-based enzyme assay for glycerophosphodiesterase family members GDE4 and GDE7

Keisuke Kitakaze^{*†}, Kazuhito Tsuboi^{*}, Maho Tsuda, Yasuhiro Takenouchi, Hironobu Ishimaru, and Yasuo Okamoto[†]

Department of Pharmacology, Kawasaki Medical School, Kurashiki, Okayama, Japan

Abstract Lysophosphatidic acid (LPA) is a lipid mediator that regulates various processes, including cell migration and cancer progression. Autotaxin (ATX) is a lysophospholipase D-type exoenzyme that produces extracellular LPA. In contrast, glycerophosphodiesterase (GDE) family members GDE4 and GDE7 are intracellular lysophospholipases D that form LPA, depending on Mg^{2+} and Ca^{2+} , respectively. Since no fluorescent substrate for these GDEs has been reported, in the present study, we examined whether a fluorescent ATX substrate, FS-3, could be applied to study GDE activity. We found that the membrane fractions of human GDE4- and GDE7-overexpressing human embryonic kidney 293T cells hydrolyzed FS-3 in a manner almost exclusively dependent on Mg^{2+} and Ca^{2+} , respectively. Using these assay systems, we found that several ATX inhibitors, including α -bromomethylene phosphonate analog of LPA and 3-carbacyclic phosphatidic acid, also potently inhibited GDE4 and GDE7 activities. In contrast, the ATX inhibitor S32826 hardly inhibited these activities. Furthermore, FS-3 was hydrolyzed in a Mg^{2+} -dependent manner by the membrane fraction of human prostate cancer LNCaP cells that express GDE4 endogenously but not by those of GDE4-deficient LNCaP cells. Similar Ca^{2+} -dependent GDE7 activity was observed in human breast cancer MCF-7 cells but not in GDE7-deficient MCF-7 cells. Finally, our assay system could selectively measure GDE4 and GDE7 activities in a mixture of the membrane fractions of GDE4- and GDE7-overexpressing human embryonic kidney 293T cells in the presence of S32826. **Key words:** These findings allow high-throughput assays of GDE4 and GDE7 activities, which could lead to the development of selective inhibitors and stimulators as well as a better understanding of the biological roles of these enzymes.

Supplementary key words enzymology • kinetics • lysophospholipid • phospholipases/D • phospholipids/biosynthesis • phospholipids/metabolism • phospholipids/phosphatidic acid • glycerophosphodiesterase • fluorescent substrate • lysophosphatidic acid



Lysophosphatidic acid (LPA) is a lipid mediator found in eukaryotic tissues and plasma (1, 2). LPA regulates various biological processes, including cell proliferation, platelet aggregation (3), smooth muscle contraction (4, 5), and malignancy and metastasis of cancers (6–8) through at least eight types of G protein-coupled receptors (2). Autotaxin (ATX) is a lysophospholipase D (lyso-PLD)-type exoenzyme that is secreted into the plasma and functions as a key enzyme that produces extracellular LPA from lysophosphatidylcholine (LPC) (9), and its activity is stimulated by divalent cations, including Mg^{2+} and Ca^{2+} (10). In humans, ATX is most abundantly expressed in the hypothalamus, retina, lung, and adipose tissues (11). In contrast, members of the glycerophosphodiesterase (GDE) family, GDE4 and GDE7, are intracellular lyso-PLD-type enzymes that hydrolyze LPC to LPA (12–14). Moreover, these GDE enzymes produce anti-inflammatory *N*-acylethanolamines from *N*-acylated lysophospholipids (15). Notably, GDE4 and GDE7 require Mg^{2+} and Ca^{2+} , respectively, for their enzymatic activities (12, 14). In humans, higher expression of GDE4 is observed in the pancreas, testis, and prostate, whereas GDE7 is abundant in the kidney, prostate, ovary, and placenta (14). Although ATX, GDE4, and GDE7 produce LPA in common, they may play unique roles because of differences in the site of action, divalent cation dependency, substrate specificity, and tissue

*For correspondence: Keisuke Kitakaze, kitakaze@med.kawasaki-m.ac.jp; Kazuhito Tsuboi, ktsuboi@med.kawasaki-m.ac.jp.

distribution. The role of each enzyme can be validated using the corresponding potent and selective inhibitors.

Recently, ATX inhibitors have gained attention owing to their association with pathological conditions, such as cancer, liver cirrhosis (16), and idiopathic pulmonary fibrosis (17). Fluorescent substrates are useful for high-throughput screening of enzyme inhibitors because of their simplicity and convenience. For ATX, compounds, such as FS-3, CPF-4, and TG-mTMP (18–20), have been reported as fluorescent substrates, and many inhibitors have been identified (21, 22). In contrast, GDE4 has been suggested to be involved in retinitis pigmentosa (23), whereas GDE7 in fatty liver (24), cancer recurrence (25), and noise-induced hearing loss (26). However, no fluorescent substrates of GDE4 or GDE7 have been reported till date, and their enzymatic activities have been measured by TLC (12, 14) and quantification of liberated choline (13), which are not suitable for high-throughput analyses.

FS-3 is a commercially available fluorescent substrate for ATX, which is characterized by a fluorescence dequenching motif. Once ATX hydrolyzes FS-3, a fluorophore that is quenched by intramolecular fluorescence resonance energy transfer to a nonfluorescent quencher becomes fluorescent, and ATX activity can be quantified in real time by temporal changes in fluorescence intensity (18). Since FS-3 is a lysophospholipid analog, we hypothesized that this compound could also act as a substrate for GDE4 and GDE7. Therefore, in the present study, we provide a real-time monitoring method using FS-3, which can selectively measure the activities of these two intracellular lysophospholipids by modifying the divalent cation being used. Using this assay system, we evaluated LPC analogs and ATX inhibitors including edelfosine (27), S32826 (28, 29), α -bromomethylene phosphonate analog of LPA (BrP-LPA) (30, 31), and 3-carbacyclic phosphatidic acid (3-ccPA) (32) and found GDE4 and GDE7 inhibitors for the first time. These findings will lead to the precise characterization of the enzymes in vitro, development of stimulators and inhibitors, and better understanding of the biological roles of GDE4 and GDE7 as well as their product LPA.

MATERIALS AND METHODS

Materials

FS-3, BrP-LPA (a mixture of two diastereomers), and oleoyl 3-ccPA were purchased from Echelon Biosciences (Salt Lake City, UT). Edelfosine (2-*O*-methyl PAF C-18) and S32826 were procured from Cayman Chemical (Ann Arbor, MI) and fluorescein from Tokyo Chemical Industry (Tokyo, Japan). Anti-FLAG M2 Ab (F1804) was purchased from Sigma-Aldrich (St. Louis, MO), anti-GDE4 Ab (27861-1-AP) from Proteintech (Rosemont, IL), anti-GDE7 Ab (HPA041148) from Atlas Antibodies (Stockholm, Sweden), anti-GAPDH Ab (MI71-3) from MBL (Tokyo, Japan), and anti-Myc-Tag Ab (2276S) from Cell Signaling Technology (Danvers, MA). We

obtained 1-oleoyl-LPC and 1-oleoyl-lysophosphatidylethanolamine (LPE) from Avanti Polar Lipids (Alabaster, AL) and DTT from Cytiva-GE Healthcare (Marlborough, MA). Nonidet P-40 (NP-40) was procured from Nacalai Tesque (Kyoto, Japan). 1-[¹⁴C]Oleoyl-LPC was enzymatically prepared from [¹⁴C]dioleoylphosphatidylcholine (American Radiolabeled Chemicals, St. Louis, MO) using *Naja mossambica mossambica* phospholipase A₂ (Sigma-Aldrich) and purified by TLC.

Cell line

Human embryonic kidney 293T (HEK293T) cells were maintained in DMEM (FUJIFILM Wako, Osaka, Japan) supplemented with 10% (v/v) FBS (Biofluids, Fleming Island, FL) and nonessential amino acids (FUJIFILM Wako). Human prostate cancer LNCaP cells were maintained in RPMI 1640 medium (FUJIFILM Wako) supplemented with 10% (v/v) FBS and nonessential amino acids. Human breast cancer MCF-7 cells were maintained in DMEM supplemented with 15% (v/v) FBS. These cell lines were cultured at 37°C in a humidified atmosphere of 5% CO₂ and 95% air.

Overexpression of enzymes

pcDNA3.1-hygro plasmid vectors harboring the complementary DNA (cDNA) of human GDE4 or GDE7 with a C-terminal FLAG tag were constructed as described previously (14). The pCAGGS vector harboring the cDNA of rat ATX with a C-terminal Myc tag (33) was gifted by Dr Junken Aoki (University of Tokyo, Tokyo, Japan). HEK293T cells were cultured to 70% confluence in a poly-L-lysine-coated dish of 100 mm. The cells were then transfected with 16 μ g of the plasmid using 40 μ l of Lipofectamine 2000 (Thermo Fisher Scientific, Waltham, MA). Control cells were also prepared using an insert-free vector. At 48 h after transfection, the cells were harvested by scraping for GDE4 and GDE7, and the conditioned medium was collected for ATX.

Genome editing

Specific guide RNA sequences were selected for human genes of GDE4 (*GDPD1*) and GDE7 (*GDPD3*) using CRISPOR (34) and cloned into the LentiGuide-Puro vector (gift from Dr Feng Zhang; Addgene; plasmid, no. 52963). The resultant LentiGuide-*GDPD1*-Puro and LentiGuide-*GDPD3*-Puro plasmids as well as lenti-Cas9-Blast (gift from Dr Feng Zhang; Addgene; plasmid, no. 52962) were used to prepare the lentivirus as described previously (35). Briefly, HEK293T cells were cotransfected with pMD2.G and psPAX2 (gifts from Dr Didier Trono [Addgene plasmids, no. 12259 and no. 12260, respectively]) together with each plasmid using Lipofectamine 2000, and lentivirus-containing conditioned media were collected. LNCaP and MCF-7 cells were transduced using the conditioned media containing lenti-Cas9-Blast lentivirus in the presence of 10 μ g/ml hexadimethrine bromide (Nacalai Tesque) and subjected to selection using 10 μ g/ml blasticidin S (FUJIFILM Wako). Cas9-expressing LNCaP and MCF-7 cells were subsequently transduced using the conditioned media containing LentiGuide-*GDPD1*-Puro and LentiGuide-*GDPD3*-Puro lentivirus, respectively, and positive clones were selected using 2 μ g/ml puromycin (FUJIFILM Wako). The clonal cell lines were isolated using the limiting dilution method. Genomic DNA from each clone was amplified and sequenced using an ABI 3130 DNA sequencer (Thermo Fisher Scientific-Applied Biosystems) for verification. The following primer pairs were used: *GDPD1*,

5'-GACAAACGCTCAGTCCAGGA-3' (forward) and 5'-AATCCCTCTCCTCCCTCCC-3' (reverse); and *GDPD3*, 5'-GAGCTTCTGTGGGAGTACGG-3' (forward) and 5'-AGCTTC-CAGATCCTGTGGG-3' (reverse).

Preparation of membrane fractions

The cells were sonicated three times for 3 s each in 50 mM Tris-HCl (pH 7.4) using an ultrasonic disruptor UD-201 (Tomy Digital Biology, Tokyo, Japan). The cell homogenates were then centrifuged at 105,000 *g* for 1 h at 4°C with Optima MAX-TL (Beckman Coulter, Brea, CA). The resultant pellets were suspended in 20 mM Tris-HCl (pH 7.4) and used as the membrane fractions. Protein concentration was determined using the Protein Assay BCA Kit (Nacalai Tesque) with BSA as a standard.

Immunoblot analysis

Immunoblot analysis was performed as described previously (36).

Fluorescence-based enzyme assay

For GDE4 and GDE7 assays, the membrane fractions (1, 5, or 6 μ g of protein) were incubated with 5 μ M FS-3 for 3 h at 37°C in 60 μ l of 50 mM Tris-HCl buffer (pH 7.4) in the presence of MgCl₂ or CaCl₂ (2 mM), or in their absence, unless otherwise stated. The fluorescence intensities were quantified at $\lambda_{\text{ex}} = 490$ nm and $\lambda_{\text{em}} = 520$ nm using a 96-well black plate and a microplate reader (Varioskan Flash; Thermo Fisher Scientific) every 10 min during the reaction (Fig. 1B) or before and after the reaction (other figures). After subtraction of the no protein control value, the amount of fluorescein released was calculated using a calibration curve, and FS-3-degrading activities were obtained. The IC₅₀ values were determined using four-parameter logistic curves. The *Z*-factor (*Z*) was calculated using the formula $Z = 1 - 3(\sigma_{\text{GDE}} + \sigma_{\text{mock}}) / (\mu_{\text{GDE}} - \mu_{\text{mock}})$, where σ and μ are the SD and means, respectively (37). *K_m* values for FS-3 were determined by Lineweaver-Burk plots using varying substrate concentrations (1–50 μ M). ATX assays were similarly performed with conditioned medium (6 μ l), except that the reaction mixture contained 50 mM Tris-HCl buffer (pH 8.0), 1 mM MgCl₂, 1 mM CaCl₂, 140 mM NaCl, 5 mM KCl, 1 mg/ml fatty acid-free BSA, and 1 mM LPC.

Radioactivity-based enzyme assay

The membrane fractions were incubated with varying concentrations (100–1,000 μ M for GDE4 assay and 10–100 μ M for GDE7 assay) of 1-[¹⁴C]oleoyl-LPC (10,000–20,000 cpm, dissolved in 5 μ l of ethanol) at 37°C for 30 min in 100 μ l of 50 mM Tris-HCl (pH 7.4) containing 2 mM of either MgCl₂ (for GDE4 assay) or 2 mM CaCl₂ (for GDE7 assay) and 100 μ M of the phosphatase inhibitor sodium orthovanadate to protect the produced 1-[¹⁴C]oleoyl-LPA from degradation (12). The reactions were terminated by the addition of 0.32 ml of a mixture of chloroform/methanol/1 M citric acid (8:4:1, by volume) with 5 mM butylated hydroxyanisole as an antioxidant. After centrifugation, 100 μ l of the lower organic phase was spotted on a silica gel-coated aluminum TLC sheet (height of 10 cm; Merck, Darmstadt, Germany), and the TLC plate was developed at 4°C for 20 min with a mixture of chloroform/methanol/90% formic acid/water (60:30:7:3, by volume) (14). The radioactivity of the substrate and product on the plate was quantified using an image analyzer (Typhoon 9400;

Cytiva-GE Healthcare), and the enzyme activity was then calculated as described previously (38).

Statistical analysis

All data are expressed as the mean \pm SD. Statistical analyses were performed by one-way ANOVA followed by Dunnett or Tukey test or two-way ANOVA with GraphPad Prism (version 8.4.3; GraphPad Software, San Diego, CA). Statistical significance was set at $P < 0.05$.

RESULTS

FS-3-degrading enzyme activity of recombinant GDE4 and GDE7

To examine whether FS-3 is a substrate of GDE4 and GDE7, we prepared HEK293T cells transiently over-expressing (O/E) the FLAG-tagged human enzymes and used their membrane fractions as enzyme sources (12, 14). Immunoblot analyses with anti-FLAG antibody confirmed the expression of each recombinant enzyme (Fig. 1A). While the predicted molecular masses from the amino acid sequences are 37.3 kDa for FLAG-tagged GDE4 and 37.7 kDa for FLAG-tagged GDE7 including potential signal peptides, their main bands appeared around 35.1 and 33.6 kDa, respectively. When the membrane fractions were allowed to react with FS-3, fluorescence intensities increased almost linearly for more than 3 h with robustness (*Z*-factor = 0.53 and 0.76 for GDE4 and GDE7, respectively) and accuracy (coefficient of variation = 13.7% and 7.6% for GDE4 and GDE7, respectively) (Fig. 1B). In contrast, the membrane fractions of the control cells showed negligible increase in fluorescence intensity. These reactions by GDE4 and GDE7 were performed with 2 mM of Mg²⁺ and Ca²⁺, respectively, which are required for the activity of the respective enzymes. Consistent with this divalent cation dependency, the activity of GDE4 was much lower with Ca²⁺ and that of GDE7 was undetectable with Mg²⁺ (Fig. 1C). The higher activity of GDE7 than that of GDE4 may reflect the difference in protein expression levels revealed by immunoblot analyses. Using varying substrate concentrations, we determined the *K_m* values of GDE4 and GDE7 for FS-3 as 18.5 and 22.2 μ M, respectively (Fig. 1D). These values were lower than those for 1-[¹⁴C]oleoyl-LPC, which were 748 μ M (for GDE4) and 55.1 μ M (for GDE7) (Fig. 1E). We next examined the effects of DTT, a sulfhydryl-reducing agent reported to stimulate GDE4 and GDE1, another member of the GDE family (12). However, this compound had only a slight effect on the FS-3-degrading activity of GDE4 and GDE7 (Fig. 1F). Since the nonionic detergent NP-40 is known to enhance the activity of several lipid-hydrolyzing enzymes, including *N*-acylethanolamine acid amidase (39, 40), we also examined the effects of this detergent. The results revealed that NP-40 enhanced the FS-3-degrading activity of GDE7 with a maximal effect at 0.1% (w/v) (5.4-fold stimulation) (Fig. 1G). In contrast, NP-40 almost

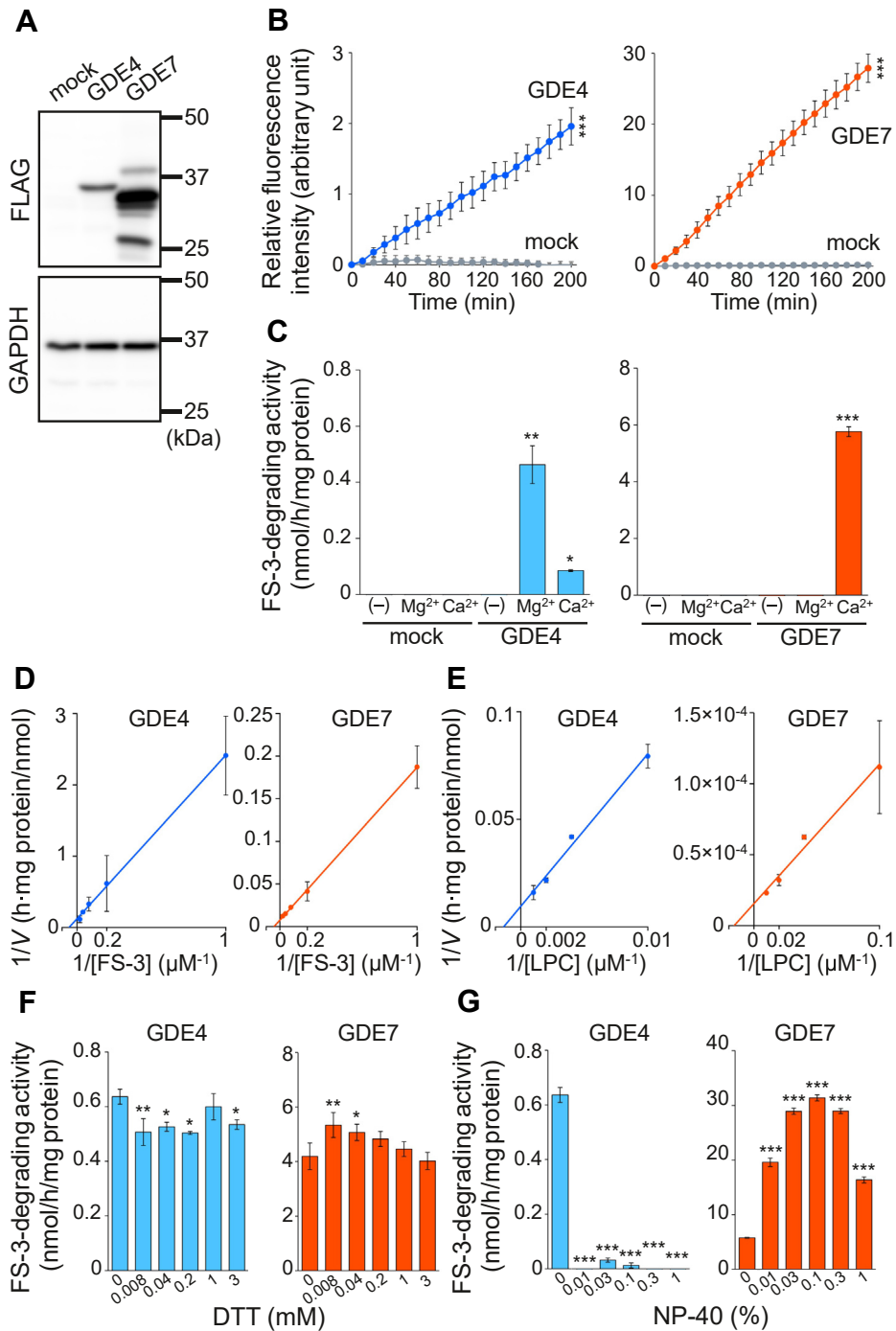


Fig. 1. FS-3-degrading enzyme activity of recombinant GDE4 and GDE7. **A:** HEK293T cells were transfected with the insert-free vector (mock) or the expression vector harboring cDNA for human GDE4 or GDE7. The membrane fractions (20 μg of protein) were analyzed by immunoblotting with anti-FLAG antibody. Anti-GAPDH antibody was used as a loading control. **B, C, F, and G:** The membrane fractions from the GDE4- (left graphs) or GDE7-overexpressing (right graphs) cells and control cells (mock) were incubated with 5 μM FS-3. The amounts of protein in the membrane fractions were 5 μg (left graphs) and 1 μg (right graphs). In **B**, fluorescence intensity was measured every 10 min, and the relative intensities are shown (mean ± SD, n = 4). In **C, F, and G**, FS-3-degrading activity was calculated by the fluorescence intensities at 0 and 180 min and expressed per 1 mg of proteins (mean ± SD, n = 3 or 4). The reaction mixtures contained 2 mM of either MgCl₂ (left graphs) or CaCl₂ (right graphs) in **B** and **D–G**, and divalent cation dependency was examined in the presence of 2 mM of MgCl₂ and CaCl₂ as well as in their absence (–) in **C**. *K_m* values (mean ± SD, n = 3) for FS-3 were determined by Lineweaver-Burk plots using varying FS-3 concentrations (1, 5, 12.5, 25, and 50 μM) in **D** and [¹⁴C]LPC concentrations (100, 250, 500, and 1,000 μM for GDE4 and 10, 25, 50, and 100 μM for GDE7) in **E**. The effects of DTT and NP-40 at indicated concentrations are shown in **F** and **G**, respectively. Two-way ANOVA (**B**) or one-way ANOVA with post hoc Dunnett test (**C, F, and G**) was conducted. **P* < 0.05, ***P* < 0.01, and ****P* < 0.001 (**B**, vs. mock; **C, F, and G**, vs. vehicle).

completely inhibited the activity of GDE4 at 0.01% (w/v). These results showed that Mg^{2+} - and Ca^{2+} -dependent hydrolyses of FS-3 are suitable for measuring the activities of recombinant GDE4 and GDE7, respectively.

Inhibitors and stimulators of GDE4 and GDE7

Using these assay systems, we evaluated LPC analogs and ATX inhibitors as potential inhibitors of GDE4 and GDE7. The results are summarized in Table 1. First, we examined LPC and LPE, endogenous substrates of these enzymes (12–14). GDE4 and GDE7 as well as ATX were inhibited by LPC in dose-dependent manners with IC_{50} values of 292 μM , 851 nM, and 3.1 μM , respectively (Fig. 2A and supplemental Fig. S1). LPE also dose-dependently inhibited GDE4 and GDE7 with IC_{50} values of 86.0 μM and 930 nM, respectively (Fig. 2B). We next used the LPC analog edelfosine, which is an inhibitor of phosphatidylinositol phospholipase C (27). Edelfosine dose-dependently inhibited GDE4 with an IC_{50} value of 17.6 μM , whereas this compound enhanced the activity of GDE7 with a maximal effect at 20 μM (3.2-fold stimulation) (Fig. 2C). We then evaluated the ATX inhibitors S32826 (28, 29), BrP-LPA (30, 31), and 3-ccPA (32). Among these three compounds, S32826 did not affect the activity of GDE4 or GDE7 (Fig. 2D). The other two compounds, BrP-LPA and 3-ccPA, inhibited GDE4 and GDE7 in a dose-dependent manner, although the inhibition of GDE4 by 3-ccPA was weaker (Fig. 2E, F). The IC_{50} values of BrP-LPA were 91.5 and 123 nM for GDE4 and GDE7, respectively, and those of 3-ccPA were 3.14 μM and 27.0 nM for GDE4 and GDE7, respectively. Thus, several compounds were found to inhibit GDE4 and GDE7 for the first time.

FS-3-degrading enzyme activity of endogenous GDE4 and GDE7

Next, we examined whether FS-3 could be hydrolyzed by endogenous enzymes. For this purpose, we established GDE4- and GDE7-KO cell lines, and the enzyme activities in the membrane fractions were compared between WT and KO cells. For GDE4, the *GDPD1* gene was genome-edited in human prostate cancer LNCaP cells, which are reported to highly express GDE4 mRNA (41), and we obtained a mutant clone with homozygous 1-bp insertion (Fig. 3A). For

GDE7, the *GDPD3* gene was edited in human breast cancer MCF-7 cells, which express GDE7 mRNA abundantly (41). This cell line is reported to be hypertriploid or hypotetraploid (42), and we obtained a GDE7-KO clone with mutations in all alleles (5-bp deletion, 8-bp deletion, and 76-bp deletion with 5-bp insertion). When the membrane fractions were analyzed by immunoblot analyses using anti-GDE4 and anti-GDE7 antibodies, each of the endogenous enzymes in WT cells was observed as a protein band with a slightly lower molecular weight than the main band obtained from the corresponding O/E cells, reflecting the size of the FLAG tag and spacer (1.2 kDa) (Fig. 3B). The bands were abolished in KO cells, confirming the absence of each enzyme. We then examined the FS-3-degrading activities using these cells. As expected, Mg^{2+} -dependent activity was observed in WT LNCaP cells, and this activity was abolished in the GDE4-KO cells (Fig. 3C). The activity with Ca^{2+} was lower than that with Mg^{2+} in the WT cells. Consistent with the results obtained with GDE7-O/E cells (Fig. 1F), NP-40 at 0.1% (w/v) increased the FS-3-degrading activity of the membrane fraction from WT MCF-7 cells by 3.3-fold (Fig. 3D). In the presence of 0.1% (w/v) NP-40, Ca^{2+} -dependent activity was observed in WT MCF-7 cells, which was decreased to 32% in the GDE7-KO cells (Fig. 3E). The activities with Mg^{2+} were much lower than those with Ca^{2+} . These results showed that FS-3 provides a useful system to measure the enzyme activities of endogenous GDE4 and GDE7, as well as their recombinant enzymes.

Selective measurement of GDE4 and GDE7 activity in the presence of both enzymes

In the assays described in Figs. 1–3, either GDE4 or GDE7 dominantly existed in the reaction mixture. We next examined whether our assay system can separately measure the activities of GDE4 and GDE7 when sufficient amounts of both enzymes are present. To this end, we mixed the membrane fractions of the GDE4-O/E and GDE7-O/E HEK293T cells and applied them to the FS-3 assay system as an enzyme source. Although intracellular membrane fractions were used, we added the ATX inhibitor S32826 to inhibit extracellular ATX activity. We found that S32826 dose-dependently inhibited the FS-3-degrading activities of

TABLE 1. Summary of stimulators and inhibitors tested

Compound	GDE4	GDE7	ATX
LPC	Inhibition (IC_{50} = 292 μM)	Inhibition (IC_{50} = 851 nM)	Inhibition (IC_{50} = 3.1 μM)
LPE	Inhibition (IC_{50} = 86.0 μM)	Inhibition (IC_{50} = 930 nM)	No data
NP-40	Inhibition (IC_{50} < 0.01%)	Stimulation (5.4-fold at 0.1%)	No data
Edelfosine	Inhibition (IC_{50} = 17.6 μM)	Stimulation (3.2-fold at 20 μM)	No data
S32826	Ineffective	Ineffective	Inhibition (IC_{50} = 198 nM)
BrP-LPA	Inhibition (IC_{50} = 91.5 nM ^a)	Inhibition (IC_{50} = 123 nM ^a)	Inhibition (IC_{50} = 22 and 165 nM ^b) (31)
3-ccPA	Inhibition (IC_{50} = 3.14 μM)	Inhibition (IC_{50} = 27.0 nM)	Inhibition (IC_{50} = 294 nM) (32)

^aValues for a mixture of two diastereomers.

^bValues for two diastereomers.

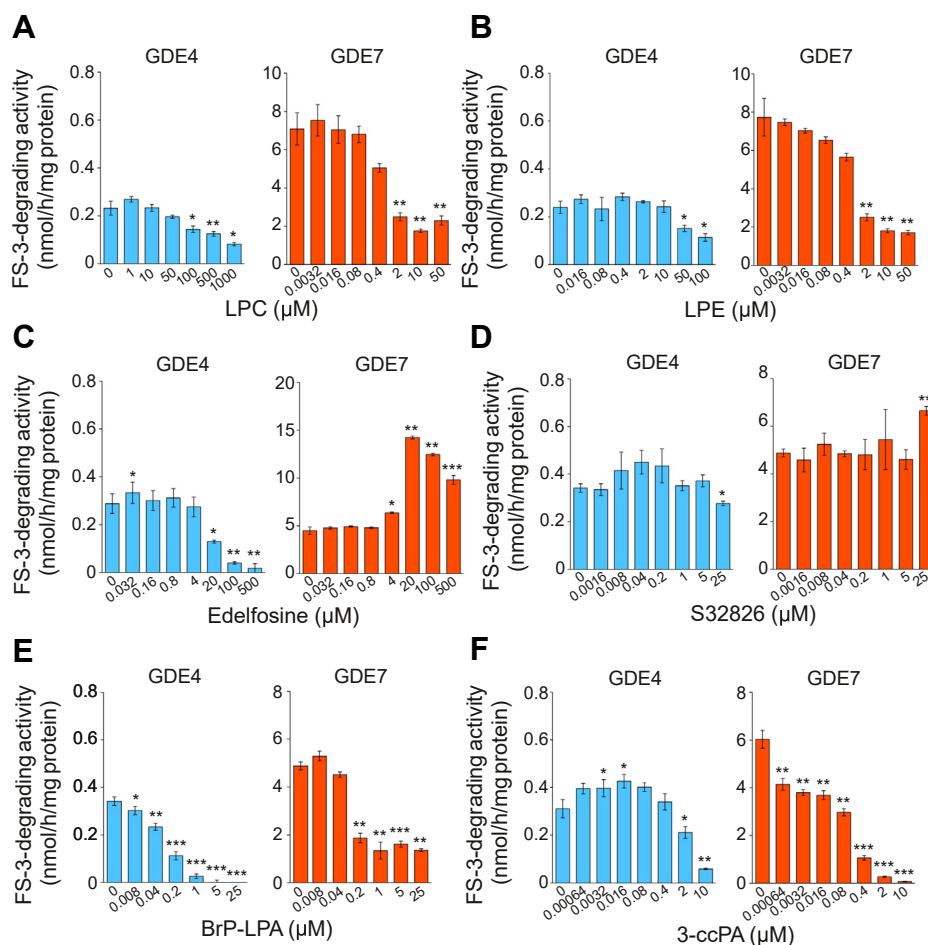


Fig. 2. Effects of natural substrates, LPC analogs, and ATX inhibitors on FS-3-degrading enzyme activity of GDE4 and GDE7. The membrane fractions from the GDE4- (left graphs) or GDE7-expressing (right graphs) HEK293T cells were incubated with 5 μ M FS-3 in the presence of 2 mM $MgCl_2$ (for GDE4) or 2 mM $CaCl_2$ (for GDE7). The amounts of protein in the membrane fractions were 5 μ g (left graphs) and 1 μ g (right graphs). The effects of LPC (5% ethanol final concentration, A), LPE (5% ethanol, B), edelfosine (C), S32826 (0.1–0.2% DMSO, D), BrP-LPA (0.1–0.2% DMSO, E), and 3-ccPA (10% methanol, F) were examined at the indicated concentrations, and FS-3-degrading activity is shown (mean \pm SD, $n = 3$ or 4). One-way ANOVA with post hoc Dunnett test was conducted. * $P < 0.05$, ** $P < 0.01$, and *** $P < 0.001$ (vs. vehicle).

rat ATX with an IC_{50} value of 198 nM (Fig. 4A) but had little effect on GDE4 or GDE7 activity (Fig. 2D). At 5 μ M, ATX activity was almost completely inhibited. Thus, we compared FS-3-degrading activities in the presence of 5 μ M S32826 among the membrane fractions of the GDE4-O/E and GDE7-O/E cells as well as their mixture. When the assays were performed in the presence of Mg^{2+} without Ca^{2+} or NP-40, the FS-3-degrading activity was solely dependent on the presence of the membrane fraction of GDE4-O/E cells (Fig. 4B). Conversely, when the reaction mixture contained Ca^{2+} and NP-40 without Mg^{2+} , the activity was completely dependent on the presence of the membrane fraction of GDE7-O/E cells. Under both conditions, the membrane fraction of the control cells exhibited negligible activity. Collectively, our assay system allowed us to selectively measure the activities of GDE4 and GDE7, even in the presence of both enzymes.

DISCUSSION

To the best of our knowledge, to date, no fluorescent substrate has been reported to measure the enzyme activity of GDE4 and GDE7. In the present study, we established a simple and convenient assay system for determining GDE4 and GDE7 activity using the fluorescent substrate FS-3 and the ATX inhibitor S32826. The K_m values of FS-3 for GDE4 and GDE7 were 18.5 and 22.2 μ M, respectively, which were lower than those of the natural substrate LPC (748 μ M for GDE4 and 55.1 μ M for GDE7), indicating the high affinity of FS-3 with these enzymes. The activities were inhibited by LPC and LPE, the natural substrates of these two enzymes, by the competition. Interestingly, FS-3 hydrolysis by GDE7 was potently inhibited by LPC with an IC_{50} value of 851 nM, which was corresponding to a K_i value of 695 nM. Since this potent inhibition cannot be explained by simple competition between both

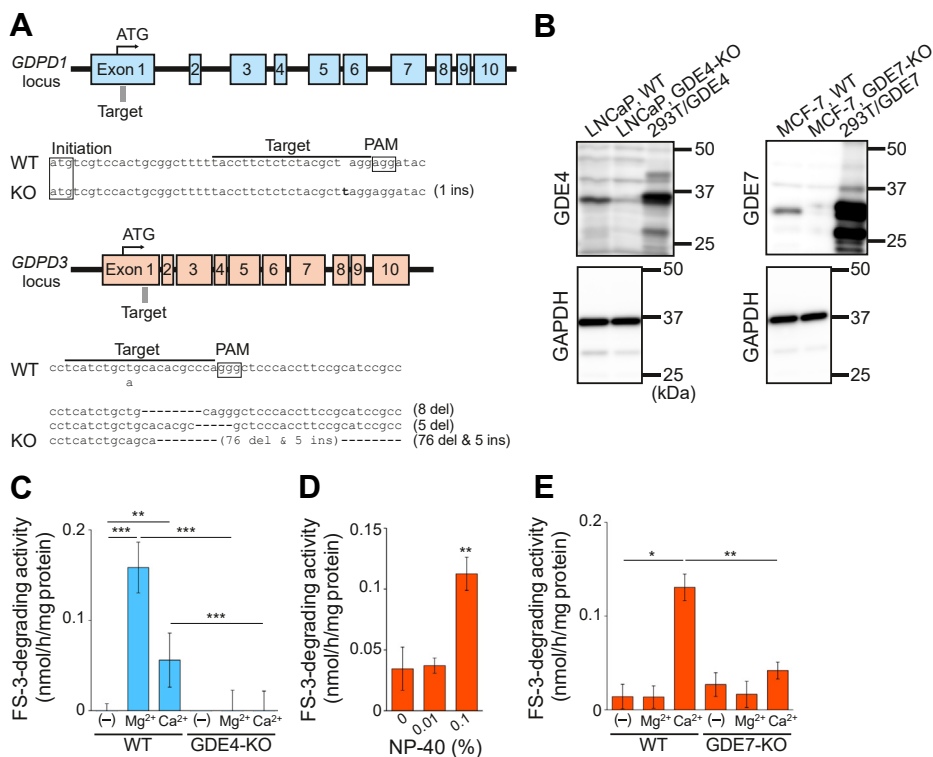


Fig. 3. FS-3-degrading enzyme activity of endogenous GDE4 and GDE7. **A:** Each vector for expressing guide RNA targeting the *GDPD1* and *GDPD3* sequences was introduced into Cas9-expressing LNCaP and MCF-7 cells, respectively. Targets of the guide RNAs are shown in each gene locus. Direct sequencing was performed after amplification of genomic DNA by PCR, and the sequences from WT and KO cells are also shown. The target sequences in WT sequences are indicated by bars, and the initiation codon and protospacer adjacent motifs (PAMs) are boxed. **B:** The membrane fractions of GDE4-KO LNCaP and GDE7-KO MCF-7 cells as well as the corresponding WT cells (15 and 20 μ g of protein for LNCaP and MCF-7 cells, respectively) were analyzed by immunoblotting with antibodies against GDE4 (for LNCaP cells) or GDE7 (for MCF-7 cells). The membrane fraction (10 μ g of protein) of human GDE4- or GDE7-expressing HEK293T cells was applied for control samples. Anti-GAPDH antibody was used as a loading control. **C:** The membrane fractions (5 μ g of protein) of WT and GDE4-KO LNCaP cells were incubated with 5 μ M FS-3 in the presence of MgCl₂ or CaCl₂ at 2 mM or in their absence (-). FS-3-degrading activity is shown (mean \pm SD, n = 4). One-way ANOVA with post hoc Tukey test was conducted. ** P < 0.01, *** P < 0.001. **D:** The membrane fractions (5 μ g of protein) of WT MCF-7 cells were incubated with 5 μ M FS-3 in the presence of 2 mM CaCl₂. Effects of the indicated concentrations of NP-40 (% w/v) on FS-3-degrading activity are shown (mean \pm SD, n = 4). One-way ANOVA with post hoc Dunnett test was conducted. ** P < 0.01 (vs. vehicle). **E:** The membrane fractions (5 μ g of protein) of WT and GDE7-KO MCF-7 cells were incubated with 5 μ M FS-3 in the presence of MgCl₂ or CaCl₂ at 2 mM or in their absence (-). FS-3-degrading activity is shown (mean \pm SD, n = 4). One-way ANOVA with post hoc Tukey test was conducted. * P < 0.05, ** P < 0.01 del, deletion; ins, insertion.

substrates, there may exist other mechanisms possibly including a detergent-like effect, product inhibition, allosteric inhibition, and an indirect effect on substrate presentation, which should be examined in future studies. This assay system exhibited a favorable Z-factor, high reproducibility, and better signal-background ratio, which suggests its robustness for high-throughput screening. Although FS-3 is characterized by a low background because of fluorescence resonance energy transfer, it is possible to be degraded by other enzymes in membrane fractions. However, FS-3 involved negligible background disturbance, even when the unpurified membrane fractions were used; this highlights the high specificity and sensitivity of this system. Previously, many ATX inhibitors have been identified by high-throughput screening using FS-3 (21, 22). Therefore, our assay system using FS-3 could possibly be used for exploring potent and selective

inhibitors of GDE4 and GDE7 as well as their stimulators in the future. However, it will be necessary to confirm whether the hit compounds exhibit similar inhibitory/stimulatory activities against natural substrates in some secondary screening.

It was reported that ATX can be inhibited by analogs of the product LPA (43), suggesting the possibility that LPA analogs inhibit GDE4 and GDE7 by the same mechanism. Using our assay system, we investigated the potential inhibition of GDE4 and GDE7 by two LPA-analog ATX inhibitors, BrP-LPA and 3-ccPA, as well as another type of ATX inhibitor, S32826. S32826 had little effect on GDE4 or GDE7 activity, indicating that it is useful for the inhibition of ATX without affecting the activity of GDE4 or GDE7. This can be attributed to the low conservation of amino acid sequences (ATX vs. GDE4 = 11.6%, ATX vs. GDE7 = 11.3%). In contrast, BrP-LPA (a mixture of two

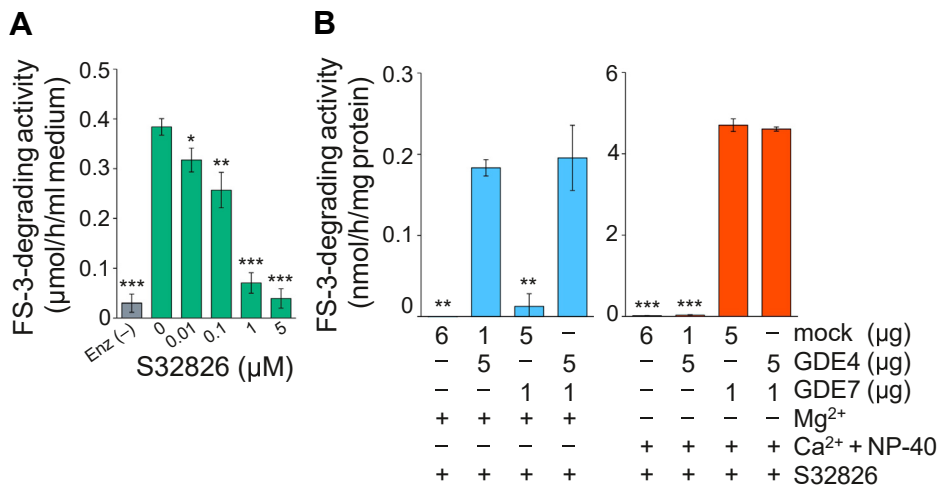


Fig. 4. Selective measurement of GDE4 and GDE7 activity in the presence of both enzymes. **A:** The FS-3-degrading activity of ATX released into the culture medium of ATX-expressing HEK293T cells was measured in the presence of the indicated concentration of S32826 (0.2% DMSO final concentration). The activity in the absence of ATX is also shown (Enz (-)). **B:** The membrane fractions (the indicated amounts of protein) of GDE4- and GDE7-expressing HEK293T cells as well as control cells (mock) were mixed and incubated with 5 µM FS-3 in the presence of 5 µM S32826. The FS-3-degrading activity of GDE4 was measured with 2 mM MgCl₂ (left graph) and that of GDE7 was determined by 2 mM CaCl₂ and 0.1% (w/v) NP-40 (right graph). Error bars indicate mean ± SD (n = 4). One-way ANOVA with post hoc Dunnett test was conducted. **P* < 0.05, ***P* < 0.01, and ****P* < 0.001 (A, vs. vehicle; B, vs. GDE4 + GDE7).

diastereomers) inhibited the enzyme activity of GDE4 and GDE7 with IC₅₀ values of 91.5 and 123 nM, respectively, which were comparable to the previously reported IC₅₀ values against ATX (22 and 165 nM for two diastereomers) using 1 µM FS-3 (31). Furthermore, 3-ccPA inhibited GDE4 and GDE7 in the micromolar and nanomolar ranges, respectively. The IC₅₀ values were 3.14 µM for GDE4 and 27.0 nM for GDE7, whereas that for ATX was reported as 294 nM using 2.5 µM of an ADMAN-LPC substrate (32). Thus, 3-ccPA was found to be a more potent inhibitor of GDE7 in contrast to GDE4 and ATX. In addition, we observed that edelfosine, an inhibitor of phosphatidylinositol phospholipase C with an IC₅₀ value of 9.6 µM (27), inhibited GDE4 with a similar IC₅₀ value (17.6 µM). From these results, we propose that our assay system is useful for screening inhibitors of GDE4 and GDE7 as well as their stimulators.

Furthermore, we showed that using our assay system, the enzyme activities of GDE4 and GDE7 could be evaluated in the presence of both the enzymes, suggesting its application to crude samples, such as extracts of various cells and tissues. The membrane fraction was used to remove liberated ATX into the culture medium. We also confirmed that the membrane-bound ATX in the membrane fraction of ATX-overexpressing HEK293T cells had only undetectable FS-3-degrading activity (data not shown). However, we added S32826 to the reaction mixture to inhibit possible contaminating ATX activity. Plasma LPA produced by ATX promotes tumor cell migration. In contrast, intracellular LPA has also been reported to affect tumor phenotypes (44–46). For example, LPA production

by acylglycerol kinase amplifies the epidermal growth factor signaling pathway in prostate cancer cells (44). In others, the level of intracellular LPA produced by GDE5 and glycerol-3-phosphate acyltransferase corresponds to tumor cell migration (46). Therefore, it may be important to determine which LPA-producing enzyme is more active in tumor tissues for diagnosis and treatment. Our enzyme assay system can be applied to gain better insights into the underlying enzymes for intracellular LPA production that affect the phenotype of tumor cells.

In conclusion, we established an assay system to selectively measure GDE4 and GDE7 activity using the fluorescent substrate FS-3. This assay system will be useful for the development of selective stimulators and inhibitors of these enzymes.

Data availability

All data supporting the findings of this study are contained in the article.

Supplemental data

This article contains [supplemental data](#).

Acknowledgments



The authors thank Rie Sugimoto for technical assistance and Editage (www.editage.com) for English language editing.

Author contributions

K. K. and K. T. conceptualization; K. K. methodology; K. K. formal analysis; K. K., K. T., and M. T. investigation; K. K. data curation; K. K. and K. T. writing—original draft; Y. T., H. I., and

Y. O. writing–review and editing; K. K. visualization; Y. O. supervision; K. K. project administration; K. K. and K. T. funding acquisition.

Author ORCIDs

Keisuke Kitakaze  <https://orcid.org/0000-0002-4852-1257>
Yasuo Okamoto  <https://orcid.org/0000-0002-2966-0577>

Funding and additional information

This work was supported by the Japan Society for the Promotion of Science KAKENHI (grant numbers: JP20K19732 to K. K. and JP20K11571 to K. T.); the Ichiro Kanehara Foundation (grant number: 2020-23 to K. K.); Teijin Pharma Limited (grant numbers: TJNS20200413014 and TJNS20210412018 to K. K. and Y. O.); Kyowa Kirin Co., Ltd. (grant number: KKCS20210402007 to K. K. and Y. O.); Bayer academic support (grant number: BASJ20210402010 to K. K. and Y. O.), and Research Project Grants from Kawasaki Medical School (grant numbers: R01S002 and R02S002 to K. K.). The funders had no role in study design, data collection, decision to publish, or preparation of the article.

Conflict of interest

K. K. and Y. O. received a grant from Teijin Pharma Limited, Bayer Yakuhin, Ltd., and Kyowa Kirin Co., Ltd. H. I. is an employee of Maruho Co., Ltd. All other authors declare that they have no conflicts of interest with the contents of this article.

Abbreviations

3-ccPA, 3-carbacyclic phosphatidic acid; ATX, autotoxin; BrP-LPA, α -bromomethylene phosphonate analog of LPA; cDNA, complementary DNA; GDE, glycerophosphodiesterase; HEK293T, human embryonic kidney 293T; LPA, lysophosphatidic acid; LPC, lysophosphatidylcholine; LPE, lysophosphatidylethanolamine; lyso-PLD, lysophospholipase D; NP-40, Nonidet P-40; O/E, overexpressing.

Manuscript received June 29, 2021, and in revised form October 8, 2021. Published, JLR Papers in Press, October 18, 2021, <https://doi.org/10.1016/j.jlr.2021.100141>

REFERENCES

1. Tokumura, A. (2004) Metabolic pathways and physiological and pathological significances of lysolipid phosphate mediators. *J. Cell Biochem.* **92**, 869–881
2. Geraldo, L. H. M., Spohr, T. C. L. S., Amaral, R. F. D., Fonseca, A. C. C. D., Garcia, C., Mendes, F. A., Freitas, C., dosSantos, M. F., and Lima, F. R. S. (2021) Role of lysophosphatidic acid and its receptors in health and disease: novel therapeutic strategies. *Signal Transduct. Target. Ther.* **6**, 45
3. Schumacher, K. A., Classen, H. G., and Späth, M. (1979) Platelet aggregation evoked in vitro and in vivo by phosphatidic acids and lysoderivatives: identity with substances in aged serum (DAS). *Thromb. Haemost.* **42**, 631–640
4. Tokumura, A., Fukuzawa, K., and Tsukatani, H. (1982) Contractile actions of lysophosphatidic acids with a chemically-defined fatty acyl group on longitudinal muscle from guinea-pig ileum. *J. Pharm. Pharmacol.* **34**, 514–516
5. Dancs, P. T., Ruisanchez, É., Balogh, A., Panta, C. R., Miklós, Z., Nüsing, R. M., Aoki, J., Chun, J., Öffermanns, S., Tigyi, G., and Benyó, Z. (2017) LPA₁ receptor-mediated thromboxane A₂ release is responsible for lysophosphatidic acid-induced vascular smooth muscle contraction. *FASEB J.* **31**, 1547–1555
6. Boucharaba, A., Serre, C-M, Grès, S., Saulnier-Blache, J. S., Bordet, J-C, Guglielmi, J., Clézardin, P., and Peyruchaud, O. (2004) Platelet-derived lysophosphatidic acid supports the progression of osteolytic bone metastases in breast cancer. *J. Clin. Invest.* **114**, 1714–1725
7. Leblanc, R., and Peyruchaud, O. (2015) New insights into the autotaxin/LPA axis in cancer development and metastasis. *Exp. Cell Res.* **333**, 183–189
8. Tang, X., Benesch, M. G. K., and Brindley, D. N. (2020) Role of the autotaxin-lysophosphatidate axis in the development of resistance to cancer therapy. *Biochim. Biophys. Acta.* **1865**, 158716
9. Zhang, X., Li, M., Yin, N., and Zhang, J. (2021) The expression regulation and biological function of autotaxin. *Cells* **10**, 939
10. Lee, J., Jung, I. D., Nam, S. W., Clair, T., Jeong, E. M., Hong, S. Y., Han, J. W., Lee, H. W., Stracke, M. L., and Lee, H. Y. (2001) Enzymatic activation of autotaxin by divalent cations without EF-hand loop region involvement. *Biochem. Pharmacol.* **62**, 219–224
11. Giganti, A., Rodriguez, M., Fould, B., Moulharat, N., Cogé, F., Chomarar, P., Galizzi, J-P, Valet, P., Saulnier-Blache, J-S, Boutin, J. A., and Ferry, G. (2008) Murine and human autotaxin α , β , and γ isoforms: gene organization, tissue distribution, and biochemical characterization. *J. Biol. Chem.* **283**, 7776–7789
12. Tsuboi, K., Okamoto, Y., Rahman, I. A. S., Uyama, T., Inoue, T., Tokumura, A., and Ueda, N. (2015) Glycerophosphodiesterase GDE4 as a novel lysophospholipase D: a possible involvement in bioactive N-acylethanolamine biosynthesis. *Biochim. Biophys. Acta.* **1851**, 537–548
13. Ohshima, N., Kudo, T., Yamashita, Y., Mariggio, S., Araki, M., Honda, A., Nagano, T., Isaji, C., Kato, N., Corda, D., Izumi, T., and Yanaka, N. (2015) New members of the mammalian glycerophosphodiester phosphodiesterase family: GDE4 and GDE7 produce lysophosphatidic acid by lysophospholipase D activity. *J. Biol. Chem.* **290**, 4260–4271
14. Rahman, I. A. S., Tsuboi, K., Hussain, Z., Yamashita, R., Okamoto, Y., Uyama, T., Yamazaki, N., Tanaka, T., Tokumura, A., and Ueda, N. (2016) Calcium-dependent generation of N-acylethanolamines and lysophosphatidic acids by glycerophosphodiesterase GDE7. *Biochim. Biophys. Acta.* **1861**, 1881–1892
15. Tsuboi, K., Uyama, T., Okamoto, Y., and Ueda, N. (2018) Endocannabinoids and related N-acylethanolamines: biological activities and metabolism. *Inflamm. Regen.* **38**, 28
16. Plesi, T., Martin, D., Kronenberger, B., Brunner, F., Köberle, V., Grammatikos, G., Farnik, H., Martinez, Y., Finkelmeier, F., Labocha, S., Ferreirós, N., Zeuzem, S., Piiper, A., and Waidmann, O. (2014) Serum autotaxin is a parameter for the severity of liver cirrhosis and overall survival in patients with liver cirrhosis – a prospective cohort study. *PLoS One* **9**, e103532
17. Oikonomou, N., Mouratis, M-A, Tzouveleki, A., Kaffe, E., Valavanis, C., Vilaras, G., Karameris, A., Prestwich, G. D., Boursos, D., and Aidinis, V. (2012) Pulmonary autotaxin expression contributes to the pathogenesis of pulmonary fibrosis. *Am. J. Respir. Cell Mol. Biol.* **47**, 566–574
18. Ferguson, C. G., Bigman, C. S., Richardson, R. D., van Meeteren, L. A., Moolenaar, W. H., and Prestwich, G. D. (2006) Fluorogenic phospholipid substrate to detect lysophospholipase D/autotaxin activity. *Org. Lett.* **8**, 2023–2026
19. Takakusa, H., Kikuchi, K., Urano, Y., Sakamoto, S., Yamaguchi, K., and Nagano, T. (2013) Design and synthesis of an enzyme-cleavable sensor molecule for phosphodiesterase activity based on fluorescence resonance energy transfer. *J. Am. Chem. Soc.* **124**, 1653–1657
20. Kawaguchi, M., Okabe, T., Okudaira, S., Nishimasu, H., Ishitani, R., Kojima, H., Nureki, O., Aoki, J., and Nagano, T. (2013) Screening and X-ray crystal structure-based optimization of autotaxin (ENPP2) inhibitors, using a newly developed fluorescence probe. *ACS Chem. Biol.* **8**, 1713–1721
21. Fells, J. I., Lee, S. C., Fujiwara, Y., Norman, D. D., Lim, K. G., Tsukahara, R., Liu, J., Patil, R., Miller, D. D., Kirby, R. J., Nelson, S., Seibel, W., Papoian, R., Parrill, A. L., Baker, D. L., et al. (2013) Hits of a high-throughput screen identify the hydrophobic pocket of autotaxin/lysophospholipase D as an inhibitory surface. *Mol. Pharmacol.* **84**, 415–424

22. Balupuri, A., Lee, M. H., Chae, S., Jung, E., Yoon, W., Kim, Y., Son, S. J., Ryu, J., Kang, D-H., Yang, Y-J., You, J-N., Kwon, H., Jeong, J-W., Koo, T-S., Lee, D-Y., *et al.* (2018) Discovery and optimization of ATX inhibitors via modeling, synthesis and biological evaluation. *Eur. J. Med. Chem.* **148**, 397–409
23. de Bruijn, S. E., Fiorentino, A., Ottaviani, D., Fanucchi, S., Melo, U. S., Corral-Serrano, J. C., Mulders, T., Georgiou, M., Rivolta, C., Pontikos, N., Arno, G., Roberts, L., Greenberg, J., Albert, S., Gilissen, C., *et al.* (2020) Structural variants create new topological-associated domains and ectopic retinal enhancer-gene contact in dominant retinitis pigmentosa. *Am. J. Hum. Genet.* **107**, 802–814
24. Key, C-C., Bishop, A. C., Wang, X., Zhao, Q., Chen, G-Y., Quinn, M. A., Zhu, X., Zhang, Q., and Parks, J. S. (2020) Human GDPD3 overexpression promotes liver steatosis by increasing lysophosphatidic acid production and fatty acid uptake. *J. Lipid Res.* **61**, 1075–1086
25. Naka, K., Ochiai, R., Matsubara, E., Kondo, C., Yang, K-M., Hoshii, T., Araki, M., Araki, K., Sotomaru, Y., Sasaki, K., Mitani, K., Kim, D-W., Ooshima, A., and Kim, S.J. (2020) The lysophospholipase D enzyme Gdpd3 is required to maintain chronic myelogenous leukaemia stem cells. *Nat. Commun.* **11**, 4681
26. Beaulac, H. J., Gilels, F., Zhang, J., Jeoung, S., and White, P. M. (2021) Primed to die: an investigation of the genetic mechanisms underlying noise-induced hearing loss and cochlear damage in homozygous Foxo3-knockout mice. *Cell Death Dis.* **12**, 682
27. Powis, G., Seewald, M. J., Gratas, C., Melder, D., Riebow, J., and Modest, E. J. (1992) Selective inhibition of phosphatidylinositol phospholipase C by cytotoxic ether lipid analogues. *Cancer Res.* **52**, 2835–2840
28. Ferry, G., Moulharat, N., Pradère, J-P., Desos, P., Try, A., Genton, A., Giganti, A., Beucher-Gaudin, M., Lonchamp, M., Bertrand, M., Saulnier-Blache, J-S., Tucker, G. C., Cordi, A., and Boutin, J. A. (2008) S32826, a nanomolar inhibitor of autotaxin: discovery, synthesis and applications as a pharmacological tool. *J. Pharmacol. Exp. Ther.* **327**, 809–819
29. Saga, H., Ohhata, A., Hayashi, A., Katoh, M., Maeda, T., Mizuno, H., Takada, Y., Komichi, Y., Ota, H., Matsumura, N., Shibaya, M., Sugiyama, T., Nakade, S., and Kishikawa, K. (2014) A novel highly potent autotaxin/ENPP2 inhibitor produces prolonged decreases in plasma lysophosphatidic acid formation in vivo and regulates urethral tension. *PLoS One.* **9**, e93230
30. Jiang, G., Xu, Y., Fujiwara, Y., Tsukahara, T., Tsukahara, R., Gajewiak, J., Tigyi, G., and Prestwich, G. D. (2007) α -Substituted phosphonate analogues of lysophosphatidic acid (LPA) selectively inhibit production and action of LPA. *ChemMedChem.* **2**, 679–690
31. Zhang, H., Xu, X., Gajewiak, J., Tsukahara, R., Fujiwara, Y., Liu, J., Fells, J. I., Perygin, D., Parrill, A. L., Tigyi, G., and Prestwich, G. D. (2009) Dual activity lysophosphatidic acid receptor pan-antagonist/autotaxin inhibitor reduces breast cancer cell migration in vitro and causes tumor regression in vivo. *Cancer Res.* **69**, 5441–5449
32. Baker, D. L., Fujiwara, Y., Pigg, K. R., Tsukahara, R., Kobayashi, S., Murofushi, H., Uchiyama, A., Murakami-Murofushi, K., Koh, E., Bandle, R. W., Byun, H-S., Bittman, R., Fan, D., Murph, M., Mills, G. B., *et al.* (2006) Carba analogs of cyclic phosphatidic acid are selective inhibitors of autotaxin and cancer cell invasion and metastasis. *J. Biol. Chem.* **281**, 22786–22793
33. Kishi, Y., Okudaira, S., Tanaka, M., Hama, K., Shida, D., Kitayama, J., Yamori, T., Aoki, J., Fujimaki, T., and Arai, H. (2006) Autotaxin is overexpressed in glioblastoma multiforme and contributes to cell motility of glioblastoma by converting lysophosphatidylcholine to lysophosphatidic acid. *J. Biol. Chem.* **281**, 17492–17500
34. Concordet, J-P., and Haeussler, M. (2018) CRISPOR: intuitive guide selection for CRISPR/Cas9 genome editing experiments and screens. *Nucleic Acids Res.* **46**, W242–W245
35. Kitakaze, K., Oyadomari, M., Zhang, J., Hamada, Y., Takenouchi, Y., Tsuboi, K., Inagaki, M., Tachikawa, M., Fujitani, Y., Okamoto, Y., and Oyadomari, S. (2021) ATF4-mediated transcriptional regulation protects against β -cell loss during endoplasmic reticulum stress in a mouse model. *Mol. Metab.* **54**, 101338
36. Takenouchi, Y., Kitakaze, K., Tsuboi, K., and Okamoto, Y. (2020) Growth differentiation factor 15 facilitates lung fibrosis by activating macrophages and fibroblasts. *Exp. Cell Res.* **391**, 112010
37. Zhang, J-H., Chung, T. D., and Oldenburg, K. R. (1999) A simple statistical parameter for use in evaluation and validation of high throughput screening assays. *J. Biomol. Screen.* **4**, 67–73
38. Tsuboi, K., Tai, T., Yamashita, R., Ali, H., Watanabe, T., Uyama, T., Okamoto, Y., Kitakaze, K., Takenouchi, Y., Go, S., Rahman, I. A. S., Houchi, H., Tanaka, T., Okamoto, Y., Tokumura, A., *et al.* (2021) Involvement of acid ceramidase in the degradation of bioactive *N*-acylethanolamines. *Biochim. Biophys. Acta.* **1866**, 158972
39. Tsuboi, K., Sun, Y-X., Okamoto, Y., Araki, N., Tonai, T., and Ueda, N. (2005) Molecular characterization of *N*-acylethanolamine-hydrolyzing acid amidase, a novel member of the cholesterylamine hydrolase family with structural and functional similarity to acid ceramidase. *J. Biol. Chem.* **280**, 11082–11092
40. Tai, T., Tsuboi, K., Uyama, T., Masuda, K., Cravatt, B. F., Houchi, H., and Ueda, N. (2012) Endogenous molecules stimulating *N*-acylethanolamine-hydrolyzing acid amidase (NAAA). *ACS Chem. Neurosci.* **3**, 379–385
41. Klijn, C., Durinck, S., Stawiski, E. W., Haverty, P. M., Jiang, Z., Liu, H., Degenhardt, J., Mayba, O., Gnad, F., Liu, J., Pau, G., Reeder, J., Cao, Y., Mukhyala, K., Selvaraj, S. K., *et al.* (2015) A comprehensive transcriptional portrait of human cancer cell lines. *Nat. Biotechnol.* **33**, 306–312
42. Rondón-Lagos, M., Verdun Di Cantogno, L., Marchiò, C., Rangel, N., Payan-Gomez, C., Gugliotta, P., Botta, C., Bussolati, G., Ramírez-Clavijo, S. R., Pasini, B., and Sapino, A. (2014) Differences and homologies of chromosomal alterations within and between breast cancer cell lines: a clustering analysis. *Mol. Cytogenet.* **7**, 8
43. van Meeteren, L. A., Ruurs, P., Christodoulou, E., Goding, J. W., Takakusa, H., Kikuchi, K., Perrakis, A., Nagano, T., and Mooleenaar, W. H. (2005) Inhibition of autotaxin by lysophosphatidic acid and sphingosine 1-phosphate. *J. Biol. Chem.* **280**, 21155–21161
44. Bektas, M., Payne, S. G., Liu, H., Goparaju, S., Milstien, S., and Spiegel, S. (2005) A novel acylglycerol kinase that produces lysophosphatidic acid modulates cross talk with EGFR in prostate cancer cells. *J. Cell Biol.* **169**, 801–811
45. Stewart, J. D., Marchan, R., Lesjak, M. S., Lambert, J., Hergenroeder, R., Ellis, J. K., Lau, C-H., Keun, H. C., Schmitz, G., Schiller, J., Eibisch, M., Hedberg, C., Waldmann, H., Lausch, E., Tanner, B., *et al.* (2012) Choline-releasing glycerophosphodiesterase EDI3 drives tumor cell migration and metastasis. *Proc. Natl. Acad. Sci. U. S. A.* **109**, 8155–8160
46. Marchan, R., Büttner, B., Lambert, J., Edlund, K., Glaeser, I., Blaszkewicz, M., Leonhardt, G., Marienhoff, L., Kaszta, D., Anft, M., Watzl, C., Madjar, K., Grinberg, M., Rempel, E., Hergenroeder, R., *et al.* (2017) Glycerol-3-phosphate acyltransferase 1 promotes tumor cell migration and poor survival in ovarian carcinoma. *Cancer Res.* **77**, 4589–4601